

**Diagnostic performances of cervical ultrasound, sestamibi scintigraphy and contrast-enhanced 18F-fluorocholine positron emission tomography in primary hyperparathyroidism.**

Vincent Boudousq, Nicolas Guignard, Olivier Gilly, Benjamin Chambert, Adel Mamou, Olivier Moranne, Mathilde Zemmour, Benjamin Lallemand

**1. Dr Vincent Boudousq**

Assistant Professor

[Vincent.boudousq@chu-nimes.fr](mailto:Vincent.boudousq@chu-nimes.fr)

Department of Nuclear Medicine, CHU Nîmes, Institut de Recherche en Cancérologie de Montpellier, INSERM U1194 UnivMontpellier, Montpellier, France

**2. Corresponding author: Dr Nicolas Guignard**

Resident

[nicolasguignard87@gmail.com](mailto:nicolasguignard87@gmail.com)

Telephone number 06 29 89 44 42

Department of Otolaryngology, Saint Jean Clinical, Saint Jean de Vedas, France

**3. Dr Olivier Gilly**

Hospital practitioner

[Olivier.Gilly@chu-nimes.fr](mailto:Olivier.Gilly@chu-nimes.fr)

Department of Metabolic and Endocrine Disease, CHU Nîmes, Univ Montpellier, Nîmes, France

**4. Dr Benjamin Chambert**

Hospital practitioner

[Benjamin.chambert@chu-nimes.fr](mailto:Benjamin.chambert@chu-nimes.fr)

Department of Nuclear Medicine, CHU Nîmes, Univ Montpellier, Nîmes, France

**5. Adel Mamou**

Biostatistician

[Mamou.ad@gmail.com](mailto:Mamou.ad@gmail.com)

R&D, NeuralX, Montpellier, France

**6. Pr Olivier Moranne**

University Professor

[Olivier.Moranne@chu-nimes.fr](mailto:Olivier.Moranne@chu-nimes.fr)

Department of Nephrology, Dialysis and Apheresis, CHU Nîmes, Univ Montpellier, Nîmes, France

**7. Mathilde Zemmour**

Resident

[Mathildezem@yahoo.fr](mailto:Mathildezem@yahoo.fr)

Department of Otolaryngology, CHU Nîmes, Univ Montpellier, Nîmes, France

**8. Dr Haitham Sharara**

Hospital practitioner

[haitham.sharara@chu-nimes.fr](mailto:haitham.sharara@chu-nimes.fr)

Department of Radiology, CHU Nîmes, Univ Montpellier, Nîmes, France

**8. Pr Benjamin Lallemand**

University Professor

[Benjamin.lallemand@chu-nimes.fr](mailto:Benjamin.lallemand@chu-nimes.fr)

Department of Otolaryngology, CHU Nîmes, Univ Montpellier, Nîmes, France

## ABSTRACT

**Purpose:** Preoperative localization of pathological parathyroids is crucial for a minimally invasive treatment of primary hyperparathyroidism (PHPT). This study compares contrast-enhanced  $^{18}\text{F}$ -fluorocholine positron emission tomography (FCH-PET/CT), cervical ultrasound (CU) and conventional scintigraphic imaging modalities (MIBI scintigraphy), combined and individually for preoperative localization of hyper-functional parathyroids in PHPT. The gold standard is histological examination.

**Methods:** Data from consecutive patients with a clinical suspicion of PHPT were retrospectively collected. All three imaging modalities were systematically performed. MIBI scintigraphy, consisted of  $^{99\text{m}}\text{Tc}$ -sestamibi/ $^{123}\text{I}$ -sodium iodide SPECT/CT,  $^{99\text{m}}\text{Tc}$ -sestamibi/ $^{123}\text{I}$ -sodium iodide planar subtraction imaging and  $^{99\text{m}}\text{Tc}$ -sestamibi planar dual-phase imaging. The ability of FCH-PET/CT, CU and MIBI scintigraphy to identify a hyper-functional parathyroid and specify the side or identify an ectopic location was noted. Patients underwent surgical exploration if at least one exam was positive. CU + MIBI scintigraphy combined was considered as a positive test if CU and MIBI scintigraphy separately showed a hyper-functional parathyroid gland on the same side, or the same ectopic location, and negative in other cases. The composite judgment criterion for pathological parathyroid combined histological analysis and normalization of PTH and calcium levels.

**Results:** 149 pathological parathyroids were found in 143 of the 144 included patients. FCH-PET/CT diagnosed 148/149 pathological parathyroids. Only four false positives and one false negative were found. The FCH-PET/CT sensitivity of 99.3% was superior to that of CU at 75.2% ( $p < 0.0001$ ), MIBI scintigraphy at 65.1% ( $p < 0.0001$ ) and CU + MIBI scintigraphy combined at 89.9%, ( $p = 0.0009$ ). 5/5 ectopic locations were diagnosed by FCH-PET/CT, 2/5 by MIBI and 0/5 by CU. Accuracy was better for FCH-PET/CT at 98% than CU at 84% ( $p < 0.0001$ ), MIBI scintigraphy at 81% ( $p < 0.0001$ ) or CU + MIBI scintigraphy at 91% ( $p < 0.0001$ ).

Among the 72 (50%) patients who had a negative CU + MIBI scintigraphy combined test, FCH-PET/CT correctly identified hyper-functional thyroids in 70 (97.2%) patients.

Average FCH-PET/CT hyperfunctional parathyroid uptake was higher than the adjacent thyroid (SULmax 6.45 vs 2.15) ( $p < 0.0001$ ).

**Conclusion:** Accuracy of FCH-PET/CT is higher than CU and MIBI scintigraphy for localization of hyper-functional parathyroids, justifying the systematic use of FCH-PET/CT as the first-line method for PHPT diagnosis.

**Keywords:** 18F-fluorocholine, primary hyperparathyroidism, parathyroid adenoma, 99mTc-sestamibi scintigraphy, cervical ultrasound

**Declarations**

*To be used for non-life science journals*

**Funding:** not applicable

**Conflicts of interest/Competing interests:** The authors declare that they have no conflicts of interest.

**Availability of data and material** (data transparency): all data and materials are available upon reasonable request to the corresponding author.

**Code availability:** not applicable

**Authors' contributions:** not applicable

**Ethics approval:** All procedures performed involving human participants were in accordance with the ethical standards of the institutional and/or national research committee and with the 1964 Helsinki declaration and its later amendments or comparable ethical standards.

**Consent to participate:** The institutional review board approved this retrospective study and the requirement to obtain informed consent was waived.

**Acknowledgments:** We thank Sarah Kabani, medical writer, for editing the manuscript.

## **INTRODUCTION**

Primary hyperparathyroidism (PHPT) is a pathology characterized by the presence of long-lasting hypercalcemia associated with inappropriate hyperparathyroidism. Idiopathic parathyroid adenomas are the most common cause of this pathology. Primary hyperparathyroidism treatment is mainly surgical, consisting in resection of pathological parathyroids (1). Previously, parathyroids were located via an exploration of the four parathyroid sites. However, the current favored technique is to identify and precisely locate the pathological parathyroids by imaging in order to propose a faster, safer targeted intervention.

For many years now, the gold standard for the preoperative localization assessment has been cervical ultrasonography (CU) combined with <sup>99m</sup>Tc-sestamibi (MIBI) scintigraphy (CU + MIBI scintigraphy) to provide supplementary anatomical and functional information. However, the results of these examinations are negative or questionable in 10 to 25% of cases (2,3), leading to further surgical explorations, the results of which are often equivocal, or to regular monitoring with repeated examinations. Defining the best diagnostic tool to minimize negative or equivocal identification is an important challenge in the surgical treatment of primary hyperparathyroidism.

<sup>18</sup>F fluorocholine (FCH) is a marker of membrane proliferation, initially used to detect cancerous tissue of prostate origin. This radio-pharmaceutical can also be very sensitively and intensely absorbed by hyper-functional parathyroid tissue. The preliminary data in the literature suggest that FCH-PET/CT would be beneficial in cases where CU + MIBI scintigraphy imaging of parathyroid adenoma gives equivocal results (4). In practice, it has quickly become obvious that FCH-PET/CT could have diagnostic values superior to CU + MIBI scintigraphy, and may soon become the gold standard as the first-line method to be used for PHPT.

To test this hypothesis, we aimed to compare the diagnostic performances of CU, MIBI scintigraphy, FCH-PET/CT and CU + MIBI scintigraphy for preoperative identification of hyper-functional parathyroids in PHPT.

## **MATERIALS AND METHODS**

This was a single center, retrospective study on patients included from July 2016 to January 2020 at the ear, nose and throat, endocrinology, and nuclear medicine departments of a French university hospital. The institutional review board approved this retrospective study and the requirement to obtain informed consent was waived.

### **Patients**

Adult patients referred for surgical consultation with PHPT and with at least one image indicating a hyper-functional parathyroid gland on at least one of the imaging modalities (CU + and/or MIBI scintigraphy + and/or FCH-PET/CT +) were included in the study between July 2016 and January 2020. Participants formed a consecutive series. PHPT were defined by hypercalcemia ( $>2.55$  mmol/L) associated with high serum parathormone (PTH) rates or inappropriate rates in the absence of vitamin D deficiency. Patients who presented associated nodular dystrophy of the thyroid were included, but those who had previously undergone surgery of the thyroid compartment were excluded, as well as any patients who had another pathology that could modify phosphocalcic metabolism such as chronic renal failure, hyper or hypovitaminosis D, sarcoidosis, multiple endocrine neoplasia or progressive neoplasia.

Over the 43-month recruiting period, 157 patients with primary hyperparathyroidism underwent all imaging studies. 144 patients fulfilled the inclusion criteria with a positive target on at least one of the imaging modalities and were operated on. Patient characteristics are described in Table 1. Briefly, we included 26 men and 118 women, with a mean age of 63 (25-92) years and a mean preoperative PTH level of 143 (39-849) pg/mL.

### **Preoperative examinations**

All patients included underwent CU, MIBI scintigraphy and FCH-PET/CT in no set order. For each examination, the presence or absence of images suggestive of hyper-functional parathyroid gland was noted along with their position in the left and right thyroid beds and ectopically. We did not differentiate the upper and lower positions. Questionable images were considered negative in the treatment decision and in the analysis of the results. The radiologists who evaluated the images were not blinded to the results of the other exams. Patients without surgical targets on the three imaging modalities were not operated on and were not included in the study.

*High resolution cervical ultrasound.* CU was performed by an experienced radiologist on an IU22 high-resolution ultrasound scan apparatus (Philips) (first used in 2012). The patient was examined supine, with the neck in extension. US was performed using high-frequency linear transducers (7– 12 MHz) for cervical examination over a field extending from the angles of the mandible to the sternum notch. The upper mediastinum was studied using an endocavitary probe for retrosternal exploration (4.5–7.2 MHz probe). Transversal and longitudinal views were obtained; images of regions of interest were recorded as video images. The parathyroid glands were sought on the posterior side of the thyroid lobes and on all cervical and upper mediastinal ectopic sites. A parathyroid was defined as pathological (adenoma or hyperplasia) if the gland was elongated or flattened, hypoechoic and separated from the thyroid parenchyma by a wall which was mobile on swallowing and well vascularized. The thyroid parenchyma was also analyzed with a detailed description of any possible dystrophy.

*Conventional scintigraphic imaging:* Conventional (i.e., non-PET/CT) scintigraphic imaging (MIBI scintigraphy) consisted of  $^{99m}\text{Tc}$ -sestamibi /  $^{123}\text{I}$  sodium iodide SPECT/CT,  $^{99m}\text{Tc}$ -sestamibi/ $^{123}\text{I}$ -sodium iodide subtraction imaging, and  $^{99m}\text{Tc}$ -sestamibi dual-phase imaging. A combined-imaging protocol was used, enabling same-day acquisition of all three modalities. Scintigraphies were performed on a Discovery 670 imager (GE Healthcare Inc.). The gamma camera was firstly equipped with a pinhole collimator allowing cervical planar acquisition and secondly with LEHR collimators allowing a cervico-thoracic planar and tomography acquisition. A matrix size of  $256 \times 256$  was used with, for dual isotope acquisition, a 10% energy window centered on the 159 keV (recommended for  $^{123}\text{I}$ ) and a 15–20% window centered around 140 keV (recommended for  $^{99m}\text{Tc}$ ). An injection of 16 MBq of  $^{123}\text{I}$  was administered, followed 2 hours later by an injection of 10 MBq/kg of  $^{99m}\text{Tc}$ -sestamibi. Five minutes after the last injection, a double isotope planar “pinhole” cervical acquisition was performed for 10 minutes. After changing the collimator, a cervico-thoracic “early” planar double isotope and a single photon emission computed tomography (SPECT) double isotope for 15 minutes combined with a cervico-thoracic computed tomography (CT) acquisition were performed. 90 minutes later, another cervical planar acquisition was done (“delayed” planar image of dual phase protocol). The following images were obtained: an “early” and “delayed” large field-of-view planar image of the neck and mediastinum (from the skull base to the heart base); a pinhole double isotope view of the thyroid bed region; and a cervico-thoracic SPECT/CT double isotope acquisition. Unless there was a contraindication, an injection of iodinated contrast medium was performed 80 seconds before the CT acquisition in order to improve the CT and the fused images visualization.

*For dual-phase imaging analysis*, early and delayed  $^{99m}\text{Tc}$ - sestamibi planar images were compared; regional uptake of  $^{99m}\text{Tc}$ - sestamibi with slower washout than thyroid tissue was considered to represent hyper-functioning parathyroid tissue.

*For dual-tracer protocols*, images were inspected visually, normalized to thyroid counts, and  $^{123}\text{I}$ -images were subtracted from the  $^{99m}\text{Tc}$ -images in the thyroid gland and surrounding soft tissue. Focal accumulation of radiopharmaceutical adjacent to the thyroid persisting after subtraction was considered suspicious for a hyper-functioning parathyroid gland.

*For SPECT/CT imaging*, a regional  $^{99m}\text{Tc}$ - sestamibi uptake not associated with thyroid tissue visualized on  $^{123}\text{I}$  or CT images was considered to represent hyper-functioning parathyroid tissue. Physiological hyper-uptake (salivary glands, inflammatory lymph nodes) was not retained.

In this study, a combined assessment of the 3 conventional scintigraphic imaging methods was done, where any positive finding according to the interpretation criteria described above was considered to represent hyper-functioning parathyroid tissue.

*$^{18}\text{F}$ -fluorocholine positron emission tomography.* FCH-PET/CT was performed 1h after intravenous injection of a dose ranging from 150 to 185 MBq of FCH, using a Discovery PET/CT 710 Elite imager (GE Healthcare Inc.). The strategy used was a CT topogram, followed by low-dose attenuation-correction CT scan, followed by PET acquisition followed by an additional intravenous contrast-enhanced diagnostic CT. In case of contraindication of contrast medium, a diagnostic CT scan was performed instead of the attenuation-correction CT scan. Acquisition protocol parameters were: Thickness: 2.5 mm; Interval: 1.25 mm; Display Field of View: 70; Tension: 120 kV; Automatical mA regulation. The acquisition was centered on the cervico-thoracic region. Iterative reconstruction of PET images was performed with the Q-Clear algorithm (GE Healthcare Inc.) to improve the signal-to-noise ratio using a Beta of 600. As contrast-enhanced CT allowed a more precise anatomic localization, unless there was a contraindication, iodinated contrast medium was injected 80 seconds before the CT acquisition in order to optimize the CT and fused images analysis. A neck or a mediastinum hyper-uptake of the radiotracer matching with a scanner image compatible with an adenoma or hyperplasia was considered as a hyper-functional parathyroid. Physiological hyper-uptake (salivary glands, inflammatory lymph nodes) was not retained. The maximum SUL (standardized uptake lean body mass for maximum) was calculated to quantify the intensity of uptake.

## **Surgery**

All patients with at least one image indicating a hyper-functional parathyroid gland on at least one of the imaging modalities were operated. The same 2cm lateral incision was used, allowing access to both upper and lower locations. If bilateral exploration was necessary, a midline incision was made. The hyper-functional parathyroid tissue was located and removed with a retro-thyroid approach under general or local anesthesia. If there was any doubt about the nature of the resected tissue, an extemporaneous anatomopathological analysis was used to confirm the presence of parathyroid tissue. Surgery could be combined with a thyroid lobectomy when there were suspect or questionable thyroid nodules on the preoperative evaluation. When the surgeon found no pathological parathyroid tissue during the surgical exploration, complete emptying of the latero-tracheal fatty cell tissue (Level VIb) was performed to limit the risk of operator-related failure to identify pathological parathyroid.

## **Statistical analysis**

The diagnostic values were defined using a composite judgement criterion, combining histological analysis (pathological tissue: adenoma / hyperplasia or normal) and the biological workup (postoperative normalization of PTH and calcium (5)). Each image evoking a hyper-functional parathyroid was considered as: true positive (TP), when confirmed as a pathological parathyroid on histological examination; or false positive (FP), if not. In the absence of an evocative image, if a surgical exploration was performed (i.e. in the event of conflicting results between the different types of images), the result was considered as: true negative (TN), if no hyper-functional parathyroid was found; or false negative (FN), if a pathological parathyroid was found. For parathyroid sites not surgically explored due to negative imaging by all imaging methods, the result was considered as: TN if a hyper-functional parathyroid was found on contralateral surgical exploration and the biological test results normalized; or impossible to conclude if no hyper-functional parathyroid was found after contralateral surgical exploration and the biological test results had not returned to normal. For each examination method, sensitivity, specificity, positive predictive and negative predictive values and their 95% confidence interval were calculated.

The accuracy, the sensitivity and the specificity of the FCH-PET/CT were compared to the performances of the CU, MIBI scintigraphy and CU + MIBI scintigraphy.

CU + MIBI scintigraphy was considered as a positive test if CU and MIBI scintigraphy separately showed a hyper-functional parathyroid gland on same side. CU + MIBI scintigraphy was considered as a negative test if there was a discrepancy



between CU and MIBI scintigraphy or if both were negative. A McNemar test for paired data was used for the comparison. A P-value lower than 0.02, adjusted for multiple comparisons with a Bonferroni correction, was considered as statistically significant.

The statistical analyses were done using the software RStudio v 1.2.5001.

The scientific committee of the Nimes University Hospital Center approved the experiments.

## **RESULTS**

For each individual patient, the pre and post-operative PTH level, result of each preoperative examination to locate the parathyroids, the histological results (including size and weight) of the parathyroids were recorded (see supplemental table 1).

### **Surgical results and anatomopathological data**

At least one hyper-functional parathyroid was found in 143 of the 144 operated patients. In total, 149 pathological parathyroids were removed: 134 patients had a single parathyroid adenoma, three patients had isolated parathyroid hyperplasia and six patients had a hyper-functional parathyroid in two sites. In one patient, no pathological parathyroid was found.

The location of these pathological glands was: the right thyroid compartment in 45.4% of cases (65/143), the left compartment in 46.9% of cases (67/143), the bilateral thyroid compartments in 4.2% of cases (6/143) and an ectopic location in 3.5% of cases (5/143): two superior mediastinal, one mid-anterior mediastinal, one left retro-esophageal and one behind the left sternoclavicular joint. No adverse events were noted during the various imaging examinations.

### **Diagnostic values with CU, MIBI scintigraphy and FCH-PET/CT**

Diagnostic values of CU, MIBI scintigraphy, CU + MIBI scintigraphy and FCH-PET/CT are given in table 2. According to histological confirmation, hyper-functional parathyroids were correctly identified (TP) in 112/149 (75%) cases by CU, in 97/149 (65%) by MIBI scintigraphy, in 148/149 (99%) by FCH-PET/CT and in 134/149 (90%) by CU + MIBI scintigraphy (reference standard).

CU wrongly diagnosed a hyper-functional parathyroid (FP) in eight cases compared with three for MIBI scintigraphy and four for FCH-PET/CT.

The FCH-PET/CT sensitivity was higher than that of CU ( $p < 0.0001$ ) and MIBI scintigraphy ( $p < 0.0001$ ), alone or combined ( $p = 0.0009$ ). Finally accuracy was better for FCH-PET/CT at 98% than CU at 84% ( $p < 0.0001$ ) and MIBI scintigraphy at 81% ( $p < 0.0001$ ) or CU + MIBI scintigraphy at 91% ( $p < 0.0001$ ).

In 72 patients (50%), the results of CU versus MIBI scintigraphy were conflicting, or found no adenomas. In these negative or equivocal identification situations, FCH-PET/CT correctly identified hyper-functional thyroids in 70 (97.2%) patients.

#### **Analysis of incorrect FCH-PET/CT results:**

FCH-PET/CT generated four FP images (patients 4, 64, 82 and 124), which may be due to localization to a thyroid nodule or lymph node. FCH-PET/CT generated one FN image (patient 87).

#### **Ectopic locations**

Five patients had a hyper-functional parathyroid in an ectopic location (two superior anterior mediastinal, one mid-anterior mediastinal, one left retro-esophageal and one behind the left sternoclavicular joint). CU did not locate pathological parathyroids in these ectopic situations (0/5 cases), and MIBI scintigraphy found only one case. In contrast, FCH-PET/CT located all of them.

#### **Analysis of the $SUL_{max}$ of hyper-functional thyroids and comparison with the physiological $SUL_{max}$ of the thyroid**

We compared the  $SUL_{max}$  of parathyroids against the adjacent thyroid parenchyma with physiological FCH uptake. The average  $SUL_{max}$  value of hyper-functional parathyroids was 6.45 (sd=3.15) compared to an average  $SUL_{max}$  value of the thyroid of 2.15 (sd=0.79). Thus the  $SUL_{max}$  value of hyper-functional parathyroids was on average 200% higher than the thyroid parenchyma,  $p < 0.0001$ . The difference in FCH uptake between the parathyroid and thyroid, combined with the spatial analysis of the distant parathyroid, facilitates the interpretation of the examination. Only Patient #31 had a parathyroid  $SUL_{max}$  lower than the thyroid ( $SUL_{max}$  4.00 versus 4.82, -17%). This patient had a previous history of Hashimoto thyroiditis with a relatively high thyroid uptake, which might explain thyroid uptake. However, there were no difficulties in diagnosing the hyper-functional parathyroid in this patient, as the parathyroid tissue was anatomically very distinct from the thyroid.

## DISCUSSION

This study was conceived due to the increasing number of centers using FCH-PET/CT for the diagnostic localization assessment of hyper-functional parathyroid glands during PHPT, despite the lack of sufficient data in the literature to justify this examination compared with the gold standard of CU + MIBI scintigraphy. The aim of work was to compare the diagnostic values of FCH-PET/CT versus the use of CU + MIBI scintigraphy. In this study, FCH-PET/CT had a sensitivity and negative predictive value of 99.0% [97%; 100%], a specificity of 97.0% [95%; 99%] and a positive predictive value of 97.4% [94%; 99%]. These diagnostic values are superior to those of CU ( $p < 0.0001$ ) and MIBI scintigraphy ( $p < 0.0001$ ), alone or combined ( $p = 0.0009$ ). These results confirm and reinforce previously published preliminary data (6-16), on a larger series of patients.

Previous publications have suggested reserving FCH-PET/CT for situations in which CU + MIBI scintigraphy has failed to detect hyper-functional thyroids. Our study demonstrates the clear diagnostic superiority of FCH-PET/CT and justifies its indication as a first-line technique in suspected PHPT.

Michaud *et al.* compared the three examinations for the preoperative evaluation of primary and secondary hyperparathyroidism in 17 patients (6). Only one case of adenoma was poorly recognized by the three imaging methods. In this limited series, the sensitivities of CU, MIBI scintigraphy and FCH-PET/CT were 42%, 83% and 96% respectively.

Another study evaluated the benefit of MIBI scintigraphy and FCH-PET/CT in 24 patients with PHPT (7). Sensitivity was significantly better with FCH-PET/CT (92%) than with MIBI scintigraphy (44-64% depending on the acquisition technique). A prospective study in 54 patients with PHPT compared CU, MIBI scintigraphy and FCH-PET/CT (8). In this study, the sensitivity of the three imaging techniques (CU, MIBI scintigraphy and FCH-PET/CT) was 69.3%, 80.7% and 100% respectively and the positive predictive values were 87.1%, 97.7% and 96.3%.

In a prospective series of 18 suspected parathyroid adenoma sites, 17 adenomas were correctly located by FCH-PET/CT with one FP, producing a sensitivity of 89% (9), comparable to the sensitivity of 90% and a positive predictive value of 100% found in another prospective series of 10 patients (10). A retrospective series of 151 patients operated for PHPT, in which FCH-PET/CT was performed at the preoperative evaluation (11) found a positive predictive value of 96.8%. Unfortunately, CU and MIBI scintigraphy were not systematically performed, preventing direct comparison.

Finally, in a recent meta-analysis on 20 studies, including a total of 796 patients, Whitman et al. reported that FCH-PET/CT had a superior sensitivity of 0.96 (0.94-0.98) compared to 0.54 (0.29-0.79) for MIBI scintigraphy ( $p < 0.001$ ). In these studies, like ours, limited to patients with primary hyperparathyroidism, FCH-PET/CT had a superior sensitivity of 0.97 (0.94-1.00) compared to 0.55 (0.32-0.78) for MIBI scintigraphy (12). In our study, MIBI scintigraphy had a sensitivity of 65.1% [57%; 72%]; this can be compared with the 10 studies (301 patients) included for comparison with MIBI scintigraphy in the meta-analysis, six (including 41% of the analyzed patients) used dual phase, dual tracer sestamibi imaging with SPECT/CT. Three articles used SPECT, two of which used use sestamibi alone, and one article did not describe the sestamibi imaging. The heterogeneity of techniques used for MIBI scintigraphy can lead to inconsistencies between the studies used for the comparison analysis. The same conventional scintigraphic imaging methods ( $^{99m}\text{Tc}$ -sestamibi SPECT/CT,  $^{99m}\text{Tc}$ -sestamibi/pertechnetate subtraction imaging, and  $^{99m}\text{Tc}$ -sestamibi dual-phase imaging ) were used by Cuderman et al. in 103 PHPT patients imaged preoperatively with a sensitivity of 65%. This sensitivity is similar to that found in our study (13).

FCH-PET/CT has numerous advantages, which justify its systematic use for the initial evaluation of hyper-functional parathyroids in patients with a clinical suspicion of PHPT. Firstly, its diagnostic values are statistically better than those of CU paired with MIBI scintigraphy, making it more reliable for the preoperative evaluation to locate hyperparathyroids. Secondly, FCH-PET/CT is more efficient and generated a lower radiation dose than MIBI scintigraphy. Indeed, FCH-PET/CT requires shorter acquisition times: 1h after injecting the tracer for FCH-PET/CT compared with over 2h for MIBI scintigraphy, and the patient spends less time under the camera and thus experiences less discomfort. FCH-PET/CT produces better image quality due to a higher spatial resolution (13-16), around 4 mm on the latest generation of PET, and a better quality mobile scanner, allowing diagnosis of smaller lesions, and increasing the sensitivity. Whole body FCH-PET/CT emits less radiation than MIBI scintigraphy, with an effective dose of 2.8mSv versus 6.8mSv (17).

Thirdly, FCH-PET/CT is the best examination for identifying ectopic adenomas. In a previous study on 54 patients, of whom six had hyper-functional thyroids in ectopic locations (two mediastinal, two in the tracheo-esophageal corner, one paravertebral and one in the mammary tissue), only FCH-PET/CT correctly identified all parathyroid adenomas (8). Similarly, in another study, one ectopic parathyroid adenoma in 10 patients was correctly identified by FCH-PET/CT and MIBI scintigraphy, but was missed by CU (10). In another study consisting of 63 patients, five patients underwent a FCH-PET/CT due to discordant CU and MIBI scintigraphy and one case of mediastinal adenoma was diagnosed, having been missed by the two other imaging techniques (18). For Taywade et al., out of seven parathyroid adenomas diagnosed, three

were ectopic parathyroids with strong FCH uptake (19). In our study, all five ectopic parathyroids from 144 patients were correctly identified with FCH-PET/CT.

Finally, FCH-PET/CT is a less operator-dependent examination and therefore more reliable than ultrasound scanning. Thyroid nodular dystrophy can easily lead to confusion between a thyroid nodule and the parathyroid on ultrasound scan, even with an experienced operator. In our experience, this confusion is much less common with an FCH-PET/CT examination. Indeed, physiological FCH uptake is low in the thyroid and almost always lower than that of the parathyroid tissue. In the rare cases of “hot” thyroid nodules, CT analysis can easily distinguish between intra-parenchymal uptake and uptake at a distance from the thyroid parenchyma. To the best of our knowledge, in the literature no association has been described between thyroiditis and strong FCH uptake of the thyroid. In our study, the only patient with a parathyroid  $SUL_{max}$  value lower than that of the thyroid had Hashimoto thyroiditis. Therefore, we would suggest that particular attention be paid when interpreting FCH-PET/CT when there is positivity for anti-thyroid antibodies and parathyroid adenoma contiguous to the thyroid, as the risk of a FN could be greater. This may also lead to problems in rare cases of intra-thyroid parathyroid adenomas.

In our study, all CUs were performed by a highly experienced operator (around 100 ultrasound parathyroid scans and 1200 thyroid ultrasound scans per year), which probably explains why the diagnostic values of the ultrasound scan are above those generally described in the literature. The MIBI scintigraphies were performed with injected iodine in our study, which increases its diagnostic values compared with other centers. The nuclear medicine physicians were experienced in analyzing FCH-PET/CT cervical images, but not for this indication. Nevertheless, the diagnostic values of FCH-PET/CT are higher than those of CU, demonstrating the less operator-dependent nature of this examination compared with the ultrasound scan.

The main disadvantages of FCH-PET/CT are the accessibility and cost. Certain authors suggest reserving FCH-PET/CT for if there is a disagreement or negative results with CU and MIBI scintigraphy (6,9,10,20-22). In our study, the results of CU and MIBI scintigraphy were discordant or negative for 50% of cases; and in 97.2% of these situations, FCH-PET/CT gave the correct location of hyper-functional parathyroids. These results reinforce the idea of using FCH-PET/CT alone as a first-line option, as suggested by Bossert et al. (23).

This work has a certain number of limitations. Our study is a single center, retrospective analysis, with the biases that this entails, especially regarding a center effect. The study only included patients with at least one positive image, probably leading to selection of patients with higher biochemical profiles and larger adenomas/hyperplastic glands, and excluding

patients with milder disease. This would inflate the diagnostic accuracy measures. The median weight of resected parathyroids was 1.12 g (0.1-7.5) compared with 0.4 g (0.1–10.9) in the 103 patients tested in a previous study (15). Nevertheless, the mean preoperative PTH level was 143 (39-849) pg/mL, similar to 145 pg/mL (40–1076 pg/mL) in that previous study. Moreover, we do not consider in this study patients affected by hyperparathyroidism with normal levels of calcium, even though patients with normal levels of calcium but with symptoms may be scheduled for surgery. This could lead to a bias in the accuracy evaluation. For some authors, FCH-PET/CT could be considered a first-line imaging technique for the identification of pathological parathyroid glands in patients with normocalcemic and hypercalcemic hyperparathyroidism, even when the parathyroid volume is small (22). Furthermore, the order of the exams was not standardized and comparisons were not performed blinded to the results of the other imaging techniques. We also did not differentiate the upper and lower localizations on the imaging results. This distinction is highly subjective and interpreter-dependent, and there is little value in distinguishing between upper or lower because the same surgical approach is used. Making this distinction would have no impact on the different diagnostic values. FCH-PET/CT imaging was performed using a 60-minute injection acquisition delay rather than 15-minute as performed by some teams, thus adenomas with fast tracer wash out may have been missed (24). This is only relevant in a very small number of cases (potentially one in our series). It is essential to pursue this work by performing a complete medico-economical study on the three techniques.

## **CONCLUSION**

The diagnostic values of FCH-PET/CT found in this study were clearly superior to those of CU and MIBI scintigraphy for preoperative localization of pathological parathyroids hyper-functional parathyroid glands in PHPT. To the best of our knowledge, with 144 patients operated, this is the biggest comparative cohort in the literature. This superiority seems related to a strong contrast between the uptake of hyper-functional parathyroids and the neighboring tissue and to a high spatial resolution allowing detection of small-sized or ectopic parathyroids, which may be missed by other imaging techniques. We suggest using FCH-PET/CT examination as a first-line treatment in preference to a CU and MIBI scintigraphy.

## **KEY POINTS**

**QUESTION:** Compare the diagnostic values of FCH-PET/CT versus CU and MIBI scintigraphy and CU + MIBI scintigraphy for the diagnostic localization assessment of hyper-functional parathyroid glands during PHPT.

**PERTINENT FINDINGS:** In this single center retrospective study of 144 operated patients, FCH PET/CT had a sensitivity and negative predictive value of over 99.0%, a specificity of 97.0% and a positive predictive value of 97.3%. These diagnostic values are superior to those of CU and MIBI scintigraphy, alone or combined; and these results confirm and reinforce previously published preliminary data, on a larger series of patients.

**IMPLICATIONS FOR PATIENT CARE:** Previous publications have suggested reserving FCH PET/CT for situations in which CU + MIBI scintigraphy has failed to detect hyper-functional thyroids, but our study demonstrates the clear diagnostic superiority of FCH-PET/CT and justify its indication as a first-line technique in suspected PHPT.

## REFERENCES

1. Fraser WD, Williams D. Hyperparathyroidism. *Lancet* (London, England). 2009;374:145–158.
2. Udelsman R, Janice LP, Sturgeon C, Young JEM, Clark OH. Surgery for asymptomatic primary hyperparathyroidism: proceedings of the third international workshop. *J Clin Endocrinol Metab*. 2009;94:366–372.
3. Civelek, AC, Ozalp E, Donovan P, Udelsman R. Prospective evaluation of delayed technetium-99m sestamibi spect scintigraphy for preoperative localization of primary hyperparathyroidism. *Surgery*. 2002;131:149-157.
4. Rep S, Lezaic L, Kocjan T, et al. Optimal scan time for evaluation of parathyroid adenoma with [(18)f]-fluorocholine PET/CT. *Radiol oncol*. 2015; 49:327–33.
5. Calzada-Nocaudie M, Chanson P, Conte-Devolx B, et al. Management of asymptomatic primary hyperparathyroidism: French society of endocrinology expert consensus. *Ann Endocrinol*. 2006;67:7-12.
6. Michaud L, Balogova S, Burgess A, et al. A pilot comparison of 18f-fluorocholine PET/CT, ultrasonography and 123I/99mTc-sestamibi dual-phase dual-isotope scintigraphy in the preoperative localization of hyperfunctioning parathyroid glands in primary or secondary hyperparathyroidism: influence of thyroid anomalies. *Medicine*. 2015;94:1701.
7. Lezaic L, Rep S, Sever MJ, Kocjan T, Hocevar M, Fettich J. <sup>18</sup>F-Fluorocholine PET/CT for localization of hyperfunctioning parathyroid tissue in primary hyperparathyroidism: a pilot study. *Eur J Nucl Med Mol Imaging*. 2014;41:2083–2089.
8. Thanseer Ntk, Bhadada SK, Sood A, et al. Comparative effectiveness of ultrasonography, 99mTc-sestamibi, and 18f-fluorocholine pet/ct in detecting parathyroid adenomas in patients with primary hyperparathyroidism. *Clin Nucl Med*. 2017;42:491–497.
9. Michaud L, Burgess A, Huchet V, et al. Is 18f-fluorocholine-positron emission tomography/computerized tomography a new imaging tool for detecting hyperfunctioning parathyroid glands in primary or secondary hyperparathyroidism? *J Clin Endocrinol Metab*. 2014;99:4531–4536.
10. Kluijfhout, Wouter P, Pasternak JD, et al. 18f fluorocholine PET/MR imaging in patients with primary hyperparathyroidism and inconclusive conventional imaging: a prospective pilot study. *Radiology*. 2017;284:460–467.
11. Hocevar M., Lezaic L, Rep S, et al. Focused parathyroidectomy without intraoperative parathormone testing is safe after pre-operative localization with <sup>18</sup>F-Fluorocholine PET/CT. *Eur J Surg Oncol*. 2017;43:133–137.
12. Whitman J, Allen I, Bergsland E, et al. Assessment and Comparison of 18 F-Fluorocholine PET and 99m Tc-Sestamibi Scans in Identifying Parathyroid Adenomas: A Meta-analysis. *J Nucl Med*. 2021; 62:1285-1291.
13. Cuderman A, Senica K, Rep S, et al. (18)F-Fluorocholine PET/CT in Primary Hyperparathyroidism: Superior Diagnostic Performance to Conventional Scintigraphic Imaging for Localization of Hyperfunctioning Parathyroid Glands. *J Nucl Med*. 2020;61:577-583.
14. Beheshti M, Hehenwarter L, Paymani Z, et al. 18f-fluorocholine pet/ct in the assessment of primary hyperparathyroidism compared with 99mTc-mibi or 99mTc-tetrofosmin spect/ct: a prospective dual-centre study in 100 patients. *Eur J Nucl Med Mol Imaging*. 2018;45:1762–1771.



15. Araz M, Soydal C, Özkan E, et al. The efficacy of fluorine-18-choline PET/CT in comparison with  $^{99m}\text{Tc}$ -MIBI SPECT/CT in the localization of a hyperfunctioning parathyroid gland in primary hyperparathyroidism. *Nucl Med Commun*. 2018;39:989–994.
16. Prabhu M, Kumari G, Damle N, et al. Assessment of the role of early dynamic PET/CT with  $^{18}\text{F}$ -fluorocholine in detection of parathyroid lesions in patients with primary hyperparathyroidism. *Nucl Med Commun*. 2018;39:1190–1196.
17. Rep S, Hocevar M, Vaupotic J, et al.  $^{18}\text{F}$ -choline PET/CT for parathyroid scintigraphy: significantly lower radiation exposure of patients in comparison to conventional nuclear medicine imaging approaches. *J Radiol Prot*. 2018;38:343–356.
18. Kluijfhout W, Vorselaars W, Vriens M, et al. Enabling minimal invasive parathyroidectomy for patients with primary hyperparathyroidism using  $\text{Tc-99m}$ -sestamibi SPECT-CT, ultrasound and first results of  $(^{18}\text{F})$ -fluorocholine PET-CT. *Eur J Radiol*. 2015;84:1745–1751.
19. Taywade S, Damle N, Behera A, et al. Comparison of  $^{18}\text{F}$ -fluorocholine Positron Emission Tomography/Computed Tomography and Four-dimensional Computed Tomography in the Preoperative Localization of Parathyroid Adenomas-initial Results. *Indian J Endocrinol Metab*. 2017;21:399–403.
20. Huber GF, Hüllner M, Schmid C, et al. Benefit of  $^{18}\text{F}$ -fluorocholine PET imaging in parathyroid surgery. *Eur Radiol*. 2018;28:2700–2707.
21. Quak E, Blanchard D, Houdu B, et al.  $^{18}\text{F}$ -choline PET/CT guided surgery in primary hyperparathyroidism when ultrasound and MIBI SPECT/CT are negative or inconclusive: the APACH<sub>1</sub> study. *Eur J Nucl Med Mol Imaging*. 2018;45:658–666.
22. Grimaldi S, Young J, Kamenicky P, et al. Challenging pre-surgical localization of hyperfunctioning parathyroid glands in primary hyperparathyroidism: the added value of  $^{18}\text{F}$ -fluorocholine PET/CT. *Eur J Nucl Med Mol Imaging*. 2018;45:1772–1780.
23. Bossert I, Chytiris S, Hodolic M, et al. PET/CT with  $^{18}\text{F}$ -choline localizes hyperfunctioning parathyroid adenomas equally well in normocalcemic hyperparathyroidism as in overt hyperparathyroidism. *J Endocrinol Invest*. 2019;42:419–426.
24. Ovčariček P, Giovanella L, Carrió Gasset I, et al. The EANM practice guidelines for parathyroid imaging. *Eur J Nucl Med Mol Imaging*. 2021;48:2801–2822.

## TABLES

**Table 1:** Characteristics of the patients operated with PHPT. Data are presented as mean (min-max) or number of patients (%)

Characteristics	n=144
Age, years	63 (25-92)
Sex: Male (M) female (F) ratio	M: 18.1% (26/144); F: 81.9% (118/144)
Preoperative parathormone, pg/mL	143 (39-849)
Postoperative parathormone, pg/mL	42 (6-126)
Number of patients with multiple operated hyper-functional thyroids	6
Number of ectopic adenomas	5
Size of resected parathyroids, mm	17 (7-35)
Weight of resected parathyroids, g	1.12 (0.1-7.5)
Mean SUL <sub>max</sub> hyper-functional parathyroids	6.46 (1.56-22.9)

**Table 2:** Diagnostic values CU, MIBI scintigraphy, CU + MIBI scintigraphy and FCH-PET/CT

<b>Imaging method</b>	<b>TP</b>	<b>FP</b>	<b>TN</b>	<b>FN</b>	<b>Accuracy</b>	<b>Se</b>	<b>Sp</b>	<b>PPV</b>	<b>NPV</b>
N = 288									
<b>FCH-PET/CT</b>	148	4	130	1	98% [96% ; 99%]	99.3% [97% ; 100%]	97.0% [95% ; 99%]	97.4% [94% ; 99%]	99.2% [96% ; 100%]
<b>CU</b>	112	8	126	37	84% [78% ; 89%]	75.2% [68% ; 82%]	94.0% [90% ; 98%]	93.3% [89% ; 98%]	77.3% [71% ; 84%]
<i>p-value</i>					<b>&lt; 0.0001</b>	<b>&lt; 0.0001</b>	0.25		
<b>MIBI scintigraphy</b>	97	3	131	52	81% [75% ; 85%]	65.1% [57% ; 72%]	97.8% [95% ; 100%]	97.0% [94% ; 100%]	71.6% [65% ; 78%]
<i>p-value</i>					<b>&lt; 0.0001</b>	<b>&lt; 0.0001</b>	0.47		
<b>CU + MIBI scintigraphy</b>	134	10	124	15	91% [86% ; 95%]	89.9% [85% ; 94%]	92.5% [88% ; 97%]	93.1% [89% ; 97%]	89.2% [84% ; 94%]
<i>p-value</i>					<b>&lt; 0.0001</b>	<b>0.0009</b>	0.09		
TP: true positive; TN: true negative; FP: false positive; FN: false negative; Se: sensitivity; Sp: specificity; PPV: positive predictive value; NPV: negative predictive value									

**Supplemental Table 1:** Results of imaging, pre- and post- operative PTH levels and histological results in 144 operated patients

Patient	Age/sex	CU	MIBI Scintigraphy	FCH-PET/CT	PTH preoperative (pg/mL)	PTH postoperative (pg/mL)	Histology	Para-thyroid size (mm) PoidSP SUL max	Para-thyroid weight (g)	Para-thyroid SUL <sub>max</sub>	Thyroid SUL <sub>max</sub>	Detectioncoefficient SUL <sub>max</sub> (%)
1	33/M	LTC	Negative	LTC	182	54	LPA	20	0.4	6.99	3.87	81
2	30/M	LTC	LTC	LTC	120	6	LPA	20	0.4	3.86	2.03	90
3	74/M	RTC	RTC	RTC	168	35	RPA	15	1.2	9.3	2.43	283
4	61/F	RTC+LTC	RTC	RTC+LTC	124	12	RPA	18	1.8	8.57+4.81	2.68	220+80
5	66/F	LTC	LTC	LTC	189	10	LPA	20	0.7	7.9	3.1	155
6	63/F	RTC	RTC	RTC	150	37	RH	20	2	13.5	2.64	411
7	47/F	RTC	RTC	RTC	95	22	RPA	25	1.8	6.17	2.7	129
8	61/F	LTC	LTC	LTC	171	25	LPA	30	1.6	5.38	1.53	252
9	53/F	LTC	LTC	LTC	113	29	LPA	24	3	4.5	1.63	176
10	78/F	LTC	LTC	LTC	59	38	LPA	17	0.6	8.76	2.64	232
11	60/F	LTC	LTC	LTC	66	24	LPA	20	1.1	6.76	4.93	37
12	54/F	LTC	LTC	LTC	64	38	LPA	13	MD	8.43	2.2	283
13	69/M	LTC	Negative	LTC	72	23	LPA	29	0.7	10.47	1.94	440
14	75/F	LTC	Negative	LTC	70	10	LPA	MD	MD	7	3.11	125
15	69/F	LTC	LTC	LTC	100	15	LH	30	2	7	1.8	289
16	63/F	RTC	Negative	RTC	140	18	RPA	8	MD	2.17	2.11	51
17	62/F	RTC	RTC	RTC	105	29	RPA	7	MD	4.2	MD	MD
18	53/F	Negative	Negative	RTC	90	18	RPA	20	0.6	15.96	0.94	1598
19	53/F	LTC	LTC	LTC	51	11	LPA	15	MD	9.64	1.87	416
20	51/F	LTC	Negative	LTC	63	12	LPA	20	0.9	4.61	2.73	69
21	50/F	LTC	Negative	LTC	119	38	LPA	MD	MD	8	1.77	352
22	60/F	LTC	Negative	LTC	118	48	LPA	10	0.5	6.85	1.09	528
23	74/F	RTC	RTC	RTC	208	44	RPA	20	MD	4.43	MD	MD
24	80/M	LTC	LTC	LTC	117	24	LPA	30	1.2	14.42	2.99	382
25	66/F	RTC+LTC	Negative	LTC	112	35	LPA	22	3	4.6	1.78	158
26	65/F	LTC	LTC	LTC	91	48	LH	15	MD	8.94	2.85	214
27	63/F	Negative	RTC+LTC	RTC+LTC	259	11	RH+LH	30+25	4.5+1.3	10.6+6.8	1.75	506+289

28	80/F	Negative	Negative	LTC	165	9	LPA	24	2	6.14	5.31	15.6
29	59/M	RTC	RTC	RTC	91	6	RPA	20	MD	4.71	2.07	128
30	66/M	Negative	RTC	RTC	263	7	RPA	24	1.4	5.37	1.45	270
31	41/F	LTC	Negative	LTC	108	37	LPA	15	0.2	4	4.82	-17
32	33/F	LTC	Negative	LTC	95	55	LPA	10	0.2	5.04	2.54	98
33	63/F	LTC	Negative	LTC	104	17	LPA	7	2	4	1.57	155
34	70/F	RTC+LTC	Negative	RTC	110	45	RPA	15	0.5	5.18	2.11	145
35	69/F	LTC	RTC+LTC	RTC	74	28	RPA	15	0.4	6.06	2.63	130
36	62/M	Negative	Negative	EL	132	16	EPA	11	MD	3.52	2.32	52
37	68/F	LTC	LTC	LTC	638	35	LPA	25	2.7	22.9	2.95	676
38	70/F	RTC	Negative	RTC	80	28	RPA	12	1	5.69	MD	MD
39	90/F	LTC	LTC	LTC	69	23	LPA	15	0.5	12.35	2.89	327
40	39/F	LTC	LTC	LTC	111	38	LPA	15	0.4	8.3	2.85	191
41	64/F	RTC	Negative	RTC	153	18	RPA	23	1.6	4.9	2.17	126
42	66/F	RTC	RTC	RTC	88	32	RPA	14	0.6	7.58	2.19	246
43	54/F	RTC	RTC	RTC	113	65	RPA	15	1.4	7.85	3.62	117
44	48/F	RTC+LTC	Negative	RTC+LTC	77	44	RH+LH	7+8	0.2+0.1	3+4.4	2.1	43+110
45	23/F	LTC	LTC	LTC	173	40	LPA	MD	0.3	11.1	1.97	463
46	71/F	RTC	RTC	RTC	119	62	RPA	18	0.4	MD	MD	MD
47	72/F	LTC	LTC	LTC	72	16	LPA	17	1	4.82	1.77	172
48	47/F	LTC	LTC	LTC	125	53	LPA	20	0.8	6.73	2.04	230
49	65/F	RTC	RTC	RTC	130	44	RPA	20	0.7	3.61	2.15	68
50	64/F	RTC	RTC	RTC	80	19	RPA	11	0.4	5.84	1.59	267
51	73/F	Negative	RTC	EL	95	42	EPA	15	0.2	7	1.78	293
52	64/M	RTC+LTC	LTC	LTC	180	64	LPA	20	1.1	7	1.79	291
53	52/F	Negative	Negative	LTC	335	15	LPA	13	0.3	3.06	1.54	99
54	37/F	LTC	Negative	LTC	150	36	LPA	30	1.1	4.65	3.34	39
55	48/F	Negative	LTC	RTC	121	32	RPA	20	MD	MD	MD	MD
56	64/F	RTC	RTC	RTC	86	55	RPA	18	0.9	8.1	2.58	214
57	78/F	Negative	RTC	RTC	135	24	RPA	23	4	5.8	2.57	126
58	87/F	RTC	RTC	RTC	281	11	RPA	9	0.2	5.55	3.04	83
59	70/F	Negative	LTC	LTC	208	8	LPA	15	0.3	5.97	2.75	237

60	43/F	Negative	LTC	RTC	147	7	LPA	14	0.1	3.99	2.06	94
61	31/M	LTC	LTC	LTC	120	28	LPA	20	0.4	3.86	MD	MD
62	56/F	LTC	Negative	LTC	124	44	LPA	10	0.2	4.02	1.06	279
63	62/F	Negative	Negative	LTC	110	36	LPA	8	0.2	6.09	MD	MD
64	49/F	RTC+LTC	RTC	RTC+LTC	56	16	RPA	14	0.4	5.08+4.09	1.74	192+135
65	56/F	RTC	RTC	RTC	100	62	RPA	18	0.9	14.5	2.83	412
66	64/F	LTC	LTC	LTC	85	62	LPA	19	0.4	3.82	1.33	187
67	61/F	RTC	RTC	RTC+LTC	110	7	RH+LH	24+11	MD	4.94+6.25	1.66	198+277
68	72/F	LTC	LTC	LTC	67	30	LPA	9	0.3	4.3	1.23	250
69	69/F	Negative	LPA	LPA	80	34	LPA	16	0.7	5.92	1.28	363
70	67/F	RTC	Negative	RTC	135	17	RPA	11	0.1	3.87	2.27	70
71	55/F	RTC	Negative	RTC	104	57	RPA	10	1.9	5.83	1.53	281
72	65/F	RTC	LTC	LTC	240	55	LPA	7	MD	2.26	1.44	57
73	62/F	Negative	Negative	LTC	100	32	LPA	10	4	5.1	1.35	278
74	59/F	LTC	Negative	LTC	106	49	LPA	12	4	MD	MD	MD
75	61/F	Negative	RTC	RTC	100	19	RPA	13	0.7	MD	MD	MD
76	55/M	Negative	LTC	LTC	89	54	LPA	15	0.1	MD	MD	MD
77	38/F	RTC	Negative	RTC	251	64	RPA	14	3	6.12	2.13	187
78	71/F	Negative	Negative	EL	143	65	EPA	23	1	4.5	1.73	160
79	71/F	RTC	Negative	RTC	144	41	RPA	12	0.2	3.8	1.7	124
80	71/F	Negative	Negative	RTC	171	60	RPA	32	0.3	3.77	1.79	111
81	79/F	Negative	Negative	EL	171	31	EPA	25	0.9	3.85	2.91	32
82	72/F	Negative	Negative	RTC	98	66	Negative	8	MD	4.15	1.62	156
83	51/M	Negative	EL	EL	92	56	EPA	18	0.5	MD	MD	MD
84	81/F	LTC	LTC	LTC	135	31	LPA	15	MD	MD	MD	MD
85	49/F	RTC	RTC	RTC	76	32	RPA	20	0.7	MD	MD	MD
86	60/F	RTC	RTC	RTC	75	31	RPA	15	0.4	5.22	1.68	211
87	50/F	RTC	Negative	Negative	75	35	RPA	10	0.1	MD	MD	MD
88	32/F	RTC	Negative	RTC	136	65	RPA	25	1.6	4.85	1.24	291
89	55/F	RTC	Negative	RTC	135	31	RPA	17	1.2	10.44	1.76	493
90	54/F	LTC	LTC	LTC	120	58	LPA	20	0.5	9.29	1.7	446
91	59/F	LTC	Negative	LTC	150	64	LPA	17	MD	4.62	1.81	155

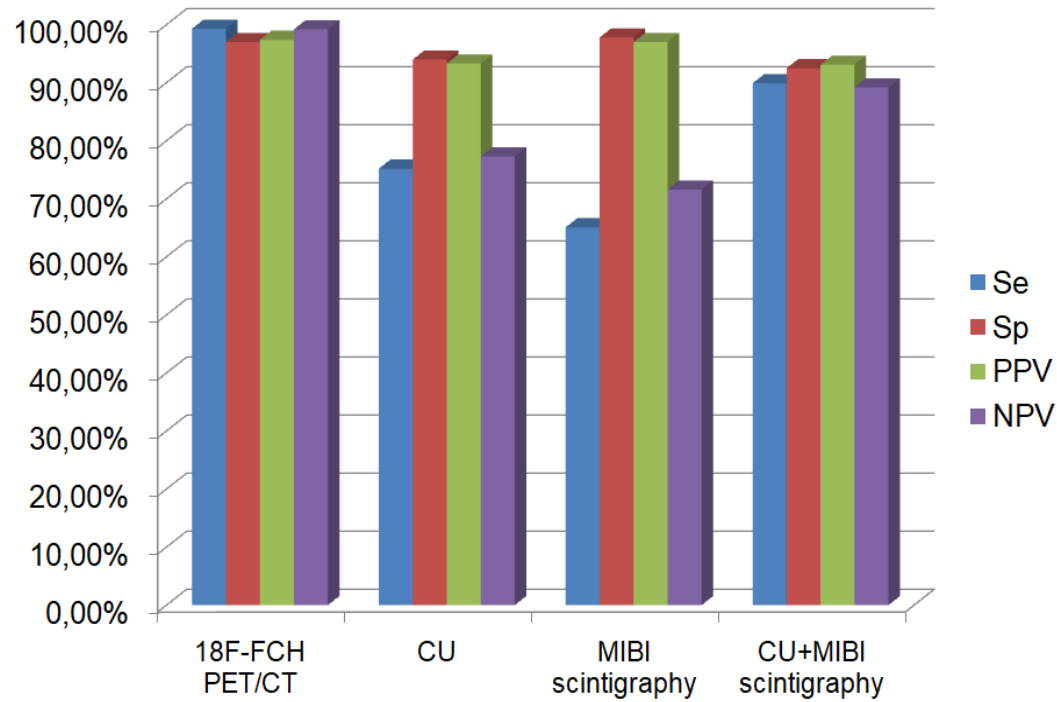
92	41/F	RTC	Negative	RTC	82	20	RPA	MD	MD	4.32	2.88	50
93	77/M	Negative	RTC	RTC	525	59	RPA	22	2.1	5.19	1.69	207
94	85/M	RTC	RTC	RTC	121	65	RPA	25	1.2	9.69	2.03	377
95	68/F	RTC	RTC	RTC	132	62	RPA	20	1.3	10.38	2.72	281
96	77/M	RTC	Negative	RTC	93	43	RPA	17	0.5	7.21	1.17	516
97	71/F	LTC	LTC	LTC	90	44	LPA	MD	MD	3.75	1.74	115
98	74/F	RTC	Negative	RTC	200	52	RPA	15	1.1	4.32	1.87	131
99	85/M	RTC	RTC	RTC	70	42	RPA	15	0.7	1.56	1.22	279
100	74/M	LTC	LTC	LTC	351	18	LPA	17	1	MD	MD	MD
101	54/F	RTC	RTC	RTC	230	11	RPA	26	4	6.94	1	594
102	40/F	RTC	RTC	RTC	74	82	RPA	20	MD	2.78	2.58	78
103	63/F	RTC	RTC	RTC	85	73	RPA	19	1,3	6.72	1.59	323
104	39/F	RTC	RTC	RTC	133	75	RPA	13	0,7	6.69	2.39	180
105	69/F	RTC	RTC	RTC	224	22	RPA	MD	MD	3.68	1.63	126
106	65/F	LTC	LTC	LTC	102	45	LPA	17	1,1	10	2.03	393
107	67/F	RTC	Negative	RTC	227	76	RPA	18	1	3.1	1.42	118
108	45/F	Negative	RTC	RTC	98	11	RPA	14	0,4	9.48	1.52	524
109	54/F	LTC	LTC	LTC	160	54	LPA	MD	MD	3.1	2.92	62
110	48/F	RTC	RTC	RTC	79	44	RPA	12	0,8	8.91	1.08	725
111	57/F	RTC	RTC	RTC	109	77	RPA	21	0,9	13.14	2.92	350
112	47/M	RTC	Negative	RTC	75	11	RPA	21	0,9	MD	MD	MD
113	82/F	LTC	LTC	LTC	178	82	LPA	MD	MD	2.85	0.89	220
114	70/F	Negative	LTC	LTC	209	126	LPA	25	1,1	6.66	1.29	416
115	70/F	LTC	LTC	LTC	93	58	LPA	12	0,4	3.99	1.58	152
116	81/F	Negative	RTC	RTC	185	52	RPA	12	0.3	2.43	1.3	87
117	60/F	RTC	Negative	RTC	82	74	RPA	8	0.4	MD	MD	MD
118	60/M	RTC	RTC	RTC	115	39	RPA	17	0.7	3.12	1.17	167
119	65/F	RTC	RTC	RTC	125	53	RPA	15	MD	2.81	1.86	51
120	69/F	LTC	LTC	LTC	105	26	LPA	19	MD	10.3	2.51	310
121	69/F	Negative	LTC	LTC	113	105	LPA	11	MD	2.93	2.88	17
122	77/F	Negative	LTC	LTC	395	46	LPA	27	MD	7.17	0.44	153
123	77/F	LTC	LTC	LTC	90	52	LPA	17	0.8	13.6	2.75	395

124	74/F	RTC	Negative	RTC+LTC	144	30	LPA	15	2	6.35	2	217
125	46/F	RTC	RTC	RTC	849	94	RPA	29	6.8	8.86	1.94	357
126	82/M	Negative	Negative	LTC	146	85	LPA	27	1.9	6.74	2.14	215
127	69/F	LTC	Negative	RTC+LTC	139	62	RPA+LPA	18+14	MD	7.24+7.11	1.35	436+427
128	77/F	RTC	RTC	RTC	39	27	RPA	15	2	3.24	1.99	63
129	53/M	RTC	RTC	RTC	158	40	RPA	35	MD	4.82	2.04	136
130	70/M	RTC	RTC	RTC	273	65	RPA	25	1.8	8.64	2.5	25
131	51/M	RTC+LTC	RTC	RTC+LTC	75	23	RPA+LPA	25+15	0.7+0.3	4.77	1.84	159
132	59/F	LTC	LTC	LTC	102	13	LPA	12	0.4	5.29	2.31	129
133	56/F	Negative	LTC	LTC	140	43	LPA	16	MD	5.52	2.13	159
134	63/M	Negative	RTC	RTC	120	33	RPA	11	0.2	4.09	1.97	108
135	75/F	LTC	LTC	LTC	149	75	LPA	17	MD	3.64	2.99	22
136	51/F	RTC	RTC	RTC	120	50	RPA	12	0.3	4.3	3.97	83
137	37/M	Negative	Negative	LPA	164	94	LPA	12	0.7	10.82	2.43	345
138	59/F	Negative	RTC	RTC	109	6	RPA	20	0.8	4.3	1.79	140
139	72/F	RTC	RTC	RTC	137	20	RPA	15	0.5	MD	MD	MD
140	66/F	LTC	LTC	LTC	250	77	LPA	12	MD	8.8	2.02	336
141	63/M	LTC	LTC	LTC	293	99	LPA	35	7.5	4.74	1.87	153
142	74/F	LTC	LTC	LTC	165	95	LPA	MD	0.6	9.79	3.25	201
143	65/F	LTC	LTC	LTC	102	95	LPA	14	MD	6.39	3.73	71
144	73/F	RTC+LTC	Negative	RTC+LTC	200	90	RPA+LPA	12+9	0.5+0.8	4.79+3.93	2.16	122+81

PTH: parathormone; M: male; F: female; LTC: hyper-functional left parathyroid thyroid compartment; RTC: hyper-functional right parathyroid thyroid compartment; LH: left parathyroid hyperplasia; RH: right parathyroid hyperplasia; EL: ectopic location; LPA: left parathyroid adenoma; RPA: right parathyroid adenoma; EPA: ectopic parathyroid adenoma; MD: missing data



## GRAPHICAL ABSTRACT



Diagnostic values CU, MIBI scintigraphy, CU+MIBI scintigraphy and  $^{18}\text{F}$ -FCH PET/CT